CrossMark

ORIGINAL ARTICLE

Structural diversity of xylans in the cell walls of monocots

Maria J. Peña[1] · Ameya R. Kulkarni[1,4] · Jason Backe[1] · Michael Boyd[2] ·
Malcolm A. O'Neill[1] · William S. York[1,3]

Abstract

Main conclusion   **Xylans in the cell walls of monocots are structurally diverse. Arabinofuranose-containing glucuronoxylans are characteristic of commelinids. However, other structural features are not correlated with the major transitions in monocot evolution.**

Most studies of xylan structure in monocot cell walls have emphasized members of the Poaceae (grasses). Thus, there is a paucity of information regarding xylan structure in other commelinid and in non-commelinid monocot walls. Here, we describe the major structural features of the xylans produced by plants selected from ten of the twelve monocot orders. Glucuronoxylans comparable to eudicot secondary wall glucuronoxylans are abundant in non-commelinid walls. However, the α-D-glucuronic acid/4-*O*-methyl-α-D-glucuronic acid is often substituted at *O*-2 by an α-L-arabinopyranose residue in Alismatales and Asparagales glucuronoxylans. Glucuronoarabinoxylans were the only xylans detected in the cell walls of five different members of the Poaceae family (grasses). By contrast, both glucuronoxylan and glucuronoarabinoxylan are formed by the Zingiberales and Commelinales (commelinids). At least one species of each monocot order, including the Poales, forms xylan with the reducing end sequence   -4)-β-D-Xyl*p*-(1,3)-α-L-Rha*p*-(1,2)-α-D-Gal*p*A-(1,4)-D-Xyl first identified in eudicot and gymnosperm glucuronoxylans. This sequence was not discernible in the arabinopyranose-containing glucuronoxylans of the Alismatales and Asparagales or the glucuronoarabinoxylans of the Poaceae. Rather, our data provide additional evidence that in Poaceae glucuronoarabinoxylan, the reducing end xylose residue is often substituted at *O*-2 with 4-*O*-methyl glucuronic acid or at *O*-3 with arabinofuranose. The variations in xylan structure and their implications for the evolution and biosynthesis of monocot cell walls are discussed.

M. J. Peña and A. R. Kulkarni contributed equally to this study.

✉ William S. York
will@ccrc.uga.edu

1   Complex Carbohydrate Research Center and US Department of Energy Bioenergy Science Center, University of Georgia, Athens, GA 30602, USA

2   Department of Plant Biology, University of Georgia, Athens, GA 30602, USA

3   Department of Biochemistry and Molecular Biology, University of Georgia, Athens, GA 30602, USA

4   Present Address: Incyte Corporation, Wilmington, DE 19803, USA

Abbreviations

AGX	Arabinoglucuronoxylan
AIR	Alcohol-insoluble residue
Ara*f*	Arabinofuranose
Ara*p*	Arabinopyranose
2AB	2-Aminobenzamide
Glc*p*A	Glucuronic acid
MeGlc*p*A	4-*O*-Methyl glucuronic acid
^{13}C NMR	Carbon nuclear magnetic resonance spectroscopy
GAX	Glucuronoarabinoxylan
GX	Glucuronoxylan

Springer

^{1}H NMR	Proton nuclear magnetic resonance spectroscopy
MALDI-TOF	MS matrix-assisted laser desorption time-of-flight mass spectrometry
Xyl$p$	Xylopyranose

Introduction

Plant cells are enclosed in a polysaccharide-rich macrostructure referred to as the cell wall. The composition of these walls varies considerably depending on the type and developmental stage of the cell that they surrounded (Fangel et al. 2012). Cells in growing tissues have non-lignified primary walls with a polysaccharide composition that differs from the lignified secondary walls of vascular and woody tissues. Additional diversity in cell wall composition also exists between different taxonomic groups, most notably in the monocots. This diverse group of land plants, which includes species of economic and ecological importance, is comprised of approximately 65,000 species that are distributed in 12 orders (Bremer et al. 2009; Givnish et al. 2010). Studies by Harris and Hartley showed that the monocots could be divided into two groups based on the presence or absence of ester-linked ferulic and coumaric acid in their primary walls (Harris and Hartley 1980). Monocots with primary walls that contain ferulate/coumarate comprise the commelinid clade (Chase et al. 1993). This clade consists of the Poales, which includes the Poaceae (grasses), Cyperaceae (sedges), and Bromeliaceae (bromeliads), together with the Zingiberales, Commelinales, and the basal Arecales (palms) (Givnish et al. 2010). The Dasypogonaceae are also considered to be commelinids but their relationship to other members of the clade has not been resolved (Chase et al. 2006). Ferulic acid esters are absent in the primary cell walls of the non-commelinid monocots, which are a paraphyletic group consisting of the Asparagales, Liliales, Pandanales, Dioscoreales, Petrosaviales, Alismatales, and Acorales. The Acorales are believed to be sister to all the monocots (Bremer et al. 2009; Givnish et al. 2010).

Commelinid and non-commelinid primary cell walls also differ in the type and abundance of their non-cellulosic polysaccharides. These differences led to the recognition of at least two types of primary wall (Bacic et al. 1988; Carpita and Gibeaut 1993; Carpita 1996; Harris et al. 1997). In the so-called type I primary walls of eudicots and non-commelinid monocots, pectin and xyloglucan account for the bulk of the non-cellulosic polysaccharides. Small amounts of xylan have also been reported to be present in these walls (Darvill et al. 1980; Zablackis et al. 1995;

Hervé et al. 2009). By contrast, glucuronoarabinoxylan (GAX) is the predominant non-cellulosic polysaccharide in the type II primary walls of the Poaceae (commelinids), which contain relatively small amounts of pectin and xyloglucan (Smith and Harris 1999; Gibeaut et al. 2005). The walls of the Poaceae are further distinguished by the presence of variable amounts of (1-3,1-4)-linked β-glucans (Carpita and Gibeaut 1993; Smith and Harris 1999). The limited data available suggest that the primary cell walls of other commelinids have characteristics of both type I and type II walls.

Xylans are the major hemicellulosic polysaccharide present in the secondary (lignified) cell walls of flowering plants. These xylans are classified according to the type and abundance of the substituents on the 1,4-linked β-D-Xyl$p$ residues of the polysaccharide backbone (Fig. 1a). Glucuronoxylans (GX), which are major components of the secondary walls of woody and herbaceous eudicots, have α-D-glucuronic acid (Glc$p$A) or 4-O-methyl α-D-glucuronic acid (MeGlc$p$A) substituents at O-2 (Ebringerova et al. 2005). The secondary wall GAX of the Poaceae and other commelinids contains α-L-Ara$f$ residues at O-3, which account for the bulk of the backbone substituents, along with a small number of Glc$p$A or MeGlc$p$A substituents at O-2. The α-L-Ara$f$ residues may be further substituted at O-2 with a α-L-Ara$f$ or a β-D-Xyl$p$ residues (Saulnier et al. 1995). The GAX in the primary walls of Poaceae typically contains more Ara$f$ substituents. The Ara$f$ residues of GAX in Poaceae primary and secondary cells walls are often esterified with ferulic or coumaric acids (Buanafina 2009).

The GX and AGX in the secondary walls of eudicots and gymnosperms have a well-defined glycosyl sequence -4)-β-D-Xyl$p$-(1,3)-α-L-Rha$p$-(1,2)-α-D-Gal$p$A-(1,4)-D-Xyl$p$ (sequence **1** in Fig. 1b) at their reducing end (Johansson and Samuelson 1977; Peña et al. 2007). This sequence is required for normal GX synthesis during secondary cell wall formation and has been proposed to have a role in regulating xylan chain length (Peña et al. 2007; York and O'Neill 2008). However, no sequence **1** has been detected at reducing end of Poaceae GAX (Kulkarni et al. 2012a). Rather, in wheat endosperm GAX, the reducing end xylose has been reported to be often substituted at O-3 with an α-L-Ara$f$ residue or at O-2 with a α-D-Glc$p$A residue (Ratnayake et al. 2014). It is not known whether sequence **1** is conserved in other commelinid and non-commelinid monocot heteroxylans.

Most studies of the composition and structure of monocot cell walls have emphasized model plants or plants of economic importance rather than phylogenetic diversity. Here, we describe the major structural features of xylans isolated from the cell walls of plants representing 10 of the 12 monocot orders. Cell walls were isolated from the entire actively growing aerial portions of each plant with a major

Fig. 1 Structural features of monocot xylans. **a** (*i*) GlcA- and MeGlcA-containing acidic side chains are present in the xylans of all monocots. (*ii*) Side chains containing Ara*p* are most abundant in the xylan of the Asparagales and Alismatales. The GlcA is 4-*O*-methylated in the Asparagales and *Eucalyptus grandis* xylans. (*iii*) Monoglycosyl Ara*f* side chains are present in GAX from commelinids. (*iv*) Side chains in which the Ara*f* is substituted were detected only in the Poales GAX. **b** Reducing end glycosyl sequences. (*v*) Sequence **1** has been detected in the xylans from numerous seed plants, except the Poaceae. (*vi*) Branched and unbranched xylosyl residues present at the reducing end of Poaceae xylans

a **Side chains identified in monocot xylans**

(i) α-D-Glc$p$A-(1→2) 4-*O*-Methyl-α-D-Glc$p$A-(1→2)-

(ii) α-L-Ara$p$-(1→2)-α-D-Glc$p$A-(1→2)- α-L-Ara$p$-(1→2)-4-*O*-Methyl-α-D-Glc$p$A-(1→2)-

(iii) α-L-Ara$f$-(1→3)-

(iv) α-L-Ara$f$-(1→2)-α-L-Ara$f$-(1→3)- β-D-Xyl$p$-(1→2)-α-L-Ara$f$-(1→3)-

b **Reducing end sequences in identified in monocot xylans**

(v) R$_1$→4)-β-D-Xyl$p$-(1→4)-β-D-Xyl$p$-(1→3)-α-LRha$p$- (1→2)-α-D-Gal$p$A-(1→4)-D-Xyl~OH

Sequence **1**

(vi) R$_1$ →4)-β-D-Xyl$p$-(1→4)-β-D-Xyl$p$-(1→4)-D-Xyl~OH

R$_1$ →4)-β-D-Xyl$p$-(1→4)-β-D-Xyl$p$-(1→4)-D-Xyl~OH
↑
R$_2$

R$_2$ = α-L-Ara$f$-(1→3)-
α-L-Ara$f$-(1→2)-α-L-Ara$f$-(1→3)-
4-*O*-Me-α-D-Glc$p$A-(1→2)-

focus on species-dependent structural variations in polysaccharide structure. In selected cases, xylans were also isolated from specific organs to examine organ-specific differences. Our data support the view that the commelinids are the only monocots to synthesize xylan with Ara$f$ substituents. These GAXs predominate in most commelinid walls, with the exception of some members of the basal Arecales, which contain mainly GX. The walls of most of the non-commelinids contain GX. Our data also demonstrate that sequence **1** is more widespread in seed plants than anticipated as it is discernible in xylans from at least one species in each monocot order. Nevertheless, sequence **1** was not detected in any of the Poaceae GAXs analyzed. Rather, the xylosyl residues at the reducing end of these GAXs were often substituted with 4-*O*-Me-Glc$p$A or with Ara$f$. Xylans lacking sequence **1** were present in some members of the Asparagales and the Alismatales. Many of these xylans contain Glc$p$A and/or MeGlc$p$A that is substituted with an α-L-Ara$p$ residue and may originate from the primary wall.

Materials and methods

Plant material and growth conditions

Actively growing stems and leaves from *Acorus americanus* (American sweet flag, Acorales), *Elodea canadensis* (Canadian waterweed, Alismatales), *Dioscorea alata* (purple yam, Dioscoreales), *Pandanus utilis* (common screwpine, Pandanales), *Agapanthus africanus* (African lily, Asparagales), *Asparagus officinalis* (asparagus, Asparagales), *Clivia miniata* (natal lily, Asparagales), *Crinum americanum* (southern swamp lily, Asparagales), *Iris germanica* (German iris, Asparagales), *Ludisia discolor* (jewel orchid, Asparagales), *Allium cepa* (onion, Asparagales), *Agave americana* (agave, Asparagales), *Caryota mitis* (fishtail palm, Arecales), *Howea forsteriana* (kentia palm, Arecales), *Rhapis excelsa* (broadleaf lady palm, Arecales), *Sabal etonia* (scrub palmetto, Arecales), *Cocus nucifera* (coconut, Arecales), *Tradescantia virginiana* (spiderwort, Commelinales), *Amomum costatum* (cardamom, Zingiberales), *Zingiber officinale* (ginger, Zingiberales), *Hedychium coronarium* (white ginger lily, Zingiberales), *Strelitzia alba* (white bird of paradise, Zingiberales), *Calathea lancifolia* (rattlesnake plant, Zingiberales), *Ctenanthe oppenheimeriana* (never–never plant, Zingiberales), *Musa* sp. (banana, Zingiberales), *Tillandsia usneoides* (Spanish moss, Bromeliaceae), and *Cyperus alternifolius* (umbrella papyrus, Cyperaceae) were obtained from the Plant Biology Greenhouse at the University of Georgia (Athens, GA).

Lemna minor (CPCC 490, Landolt clone 8434, Alismatales) was obtained from the Canadian Phycological Culture Centre (University of Waterloo, Canada). *Spirodela polyrhiza* (ID7498) was obtained from Joachim

Messing (Waksman Institute of Microbiology, Rutgers University, New Jersey, United States of America). Duckweeds were grown on Schenk and Hildebrandt basal salts (1.6 g L^{-1}), pH 5.8, containing sucrose (10 g L^{-1}), morpholinoethanesulfonic acid (0.5 g L^{-1}), and agar (8 g L^{-1}) in a controlled environmental growth chamber (Adaptis A1000, Conviron, Winnipeg, Canada) at 19 and 15 °C with a 14-h light and 10-h dark cycle, respectively, with a light intensity of 120 μmol quanta m^{-2} s^{-1}, and 70 % relative humidity.

Stems and leaves of mature *Miscanthus x giganteus* (giant miscanthus), *Brachypodium distachyon*, and *Setaria italica* (Poaceae) were obtained from the Plant Biology Greenhouse at the University of Georgia (Athens, GA). *Oryza sativa* (rice, Poaceae) straw was obtained from Wayne Parrot at the University of Georgia. The air-dried stems and leaves were Wiley-milled (−20/+80 mesh) and kept at room temperature. *Panicum virgatum* cultivar Alamo (switchgrass, Poaceae) was obtained from the Samuel Roberts Noble Foundation (Ardmore, Oklahoma, USA). The biomass was milled using a Hammer mill with a "1" screen and then ground in a Wiley mill using a 1-mm screen. The milled material was sieved to −20/+80 mesh.

Eucalyptus grandis wood was obtained from Will Rottman (Arborgen, Ridgeville, SC, USA), and *Orontium aquaticum* (golden club, Alismatales) was collected from Newton Creek, Dothan, Alabama USA, by Ron Clay of the CCRC. *Ananas comosus* (pineapple, Bromeliaceae), *Tulipa* sp. (tulip, Liliacea), and *Alstroemeria* sp. (Peruvian lily, Liliales) and shoots of *Asparagus officinalis* (asparagus, Asparagales) were obtained from a local grocery store.

Preparation of cell walls

Cell walls were prepared as their alcohol-insoluble residues (AIRs) by homogenizing suspensions of the plant material in aq. 80 % (v/v) EtOH with a Polytron tissue disruptor (Kinematica, Switzerland). To facilitate labeling of grass cell walls with 2-aminobenzamide (2AB), the homogenized material was ball-milled for 16 h at 4 °C and 90–100 rpm in aq. 80 % EtOH (v/v) using ¼ in. zirconium grinding media (U.S. Stoneware, East Palestine, OH). This procedure reduced the AIR particle size to <50 μm. The AIRs were then washed with absolute EtOH, with MeOH:CHCl$_3$ (1: 1 v/v), and with acetone and then vacuum-dried at room temperature.

2-Aminobenzamide labeling of the reducing glycoses present in AIR

The ball-milled AIR (100–200 mg) from the five grasses was suspended in DMSO: HOAc (70:30 v/v) containing sodium cyanoborohydride (1 M) and 2AB (0.5 M) and

kept for 16 h at 65 °C (Bigge et al. 1995). The suspensions were then dialyzed against deionized water (3500 molecular weight cut-off tubing) and lyophilized.

Sequential extraction of AIR

The AIR and the 2AB-labeled AIR (0.5 g) were sequentially extracted with 50 mM ammonium oxalate (35 mL) and then with 1 M KOH containing 1 % (w/v) NaBH$_4$. The 1 M KOH-soluble extracts were neutralized with HOAc, dialyzed (3500 MWCO tubing) against deionized water, and then lyophilized.

Generation of xylo-oligosaccharides by endoxylanase treatment of the 1 M KOH-soluble material

The 1 M KOH-soluble materials (∼20 mg) were suspended in 50 mM ammonium formate, pH 5, and treated for 24 h at 37 °C with *endo*xylanase (3.5 unit, *Trichoderma viride* M1, Megazyme, Wicklow, Ireland). The insoluble residues were removed by centrifugation and EtOH then added to the supernatant to a final concentration of 60 % (v/v). The mixture was kept for 24 h at 4 °C. The precipitate that formed was removed by centrifugation and the soluble material lyophilized. The xylo-oligosaccharides were purified by size exclusion chromatography (SEC) using a Superdex-75 HR10/30 column (GE Healthcare) and a Dionex Ultimate 3000 HPLC equipped with a Shodex RI-101 refractive index detector and a fluorescence detector. The column was eluted with 50 mM ammonium formate, pH 5, and the fraction containing xylo-oligosaccharides were collected and freeze-dried. The xylo-oligosaccharides were analyzed by MALDI-TOF MS spectrometry and NMR spectroscopy.

The 2AB-labeled xylo-oligosaccharides generated by enzymatic digestion of the 1 M KOH-soluble materials from the 2AB-labeled AIR were partially purified by SEC as described above. Acidic and neutral 2AB-labeled xylo-oligosaccharides were separated by solid-phase extraction (SPE) using graphitized carbon cartridges (Packer et al. 1998). The oligosaccharides were eluted with a series of increasing concentrations of acetonitrile (10 % (v/v) acetonitrile to 80 % (v/v) acetonitrile). Most of the acidic 2AB-labeled xylo-oligosaccharides were eluted with 40 % (v/v) acetonitrile.

Matrix-assisted laser desorption/ionization time-of-flight mass spectrometry (MALDI-TOF MS)

Positive ion MALDI-TOF mass spectra were recorded using a Bruker LT MALDI-TOF mass spectrometer interfaced to a Bruker Biospectrometry workstation (Bruker

Daltonics, http://www.bdal.com) as described (Mazumder and York 2010).

Electrospray ionization mass spectrometry (ESI MS)

Materials enriched in acidic or neutral 2AB-labeled xylo-oligosaccharides (~1 mg) were dissolved in dry DMSO (0.2 mL) and per-*O*-methylated and isolated as described (Mazumder and York 2010). The per-*O*-methylated xylo-oligosaccharides were then analyzed by positive ion ESI MS using a ThermoScientific LTQ XL mass spectrometer (Thermo Scientific, http://www.thermoscientific.com) as described (Mazumder and York 2010).

NMR spectroscopy

Native and 2AB-labeled xylo-oligosaccharides were dissolved in D_2O (3–5 mg in 0.3 mL, 99.9 %; Cambridge Isotope Laboratories). One- and two-dimensional NMR spectra were recorded at 298 K with a Varian Inova NMR spectrometer operating at 600 MHz and equipped with a 5-mm NMR cold probe (Agilent, Santa Clara, CA). Homonuclear (gCOSY, TOCSY, and ROESY) and the heteronuclear (gHSQC and gHMBC) experiments were recorded using standard Varian pulse programs. Chemical shifts were measured relative to internal acetone at δ_H 2.225 and δ_C 30.89. Data were processed using MestRe-Nova software (Universidad de Santiago de Compostela, Spain).

Results

The cell walls of commelinid and non-commelinid monocots contain structurally distinct heteroxylans

To determine the species-dependent differences in xylan structure, cell walls were isolated from the entire actively growing aerial portions of plants representing 10 (Poales, Zingiberales, Commelinales, Arecales, Asparagales, Liliales, Pandanales, Dioscoreales, Alismatales, and Acorales) of the 12 orders of monocots. Material enriched in xylan was then solubilized by treating the depectinated AIR with 1 M KOH. The xylans were fragmented with endoxylanase and the resulting xylo-oligosaccharides isolated by SEC and structurally characterized using mass spectrometry and NMR spectroscopy. MALDI-TOF MS provides information regarding the number and identity of the glycosyl residues (pentose, hexose, or hexuronic acid) in each oligosaccharide. 1D and 2D ^{1}H NMR spectroscopy of the oligosaccharides provides information about the glycosyl composition, linkage, and sequence of each

oligosaccharide. Assignment of NMR resonances was facilitated by comparison with previously published chemical shift data for the ^{1}H and ^{13}C resonances of the residues in oligosaccharides prepared from structurally diverse heteroxylans (Peña et al. 2007; Kulkarni et al. 2012a).

The commelinid clade is resolved into two groups on the basis of their MALDI-TOF MS xylo-oligosaccharide profiles. In the first group, which includes *Panicum virgatum*, *Brachypodium distachyon*, *Oryza sativa*, *Miscanthus × giganteus*, and *Setaria italica* (Poaceae), *Calathea lancifolia* and *Ctenanthe oppenheimiana* (Marantaceae), and *Amomum costatum* and *Zingiber officinialis* (Zingiberaceae) (see Fig. 2, Supplementary Fig. S1), the spectra are dominated by [M + Na]$^+$ ions (*m/z* 701, 833, 965, and 1097), corresponding to oligosaccharides containing from 5 to 8 pentosyl residues. Ions originating from oligosaccharides containing a MeGlc*p*A (M) residue (e.g., P$_4$M at *m/z* 759 and P$_5$M at *m/z* 891) were present at much lower abundance (Fig. 2, Supplementary Fig. S1). These types and abundance of neutral and acidic oligosaccharides are the expected products of xylanase fragmentation of GAX that contain only a few MeGlc*p*A residues. Such GAXs are the predominant hemicellulose in the cell walls of the Poaceae (Poales) (Ebringerova et al. 2005). The MALDI-TOF MS spectra of the xylo-oligosaccharides from the second group of commelinids (Fig. 2, Supplementary Fig. S1), which includes *Cyperus alternifolius* (Cyperaceae), *Ananas Comosus* and *Tillandsia usneoides* (Bromeliaceae), *Musa* sp. (Musaceae), *Tradescantia virginiata* (Commelinaceae), and *Sabal etonia*, *Cocos Nucifera*, *Caryota mitis*, and *Rhapis excelsa* (Arecaceae), were dominated by [M + Na]$^+$ ions (*m/z* 759, 891, 1023, and 1155) and [M − H + 2Na]$^+$ ions (*m/z* 781, 913, 1045, 1177), which correspond to oligosaccharides composed of a single MeGlc*p*A residue and from 4 to 7 pentosyl residues (P$_4$M–P$_7$M).

The MALDI-TOF MS xylo-oligosaccharide profiles of all the non-commelinids contained ions that correspond to acidic oligosaccharides composed of 4-6 xylosyl residues and one uronic acid (Fig. 2, Supplementary Fig. S1). Typically, most of the Glc*p*A residues were 4-*O*-methylated. However, xylo-oligosaccharides from *Crinum americanum* (Amaryllidaceae), *Ludisia discolor* (Orchidaceae), *Iris germanica* (Iridaceae), *Orontium aquaticum* and *Spirodela polyrhiza* (Araceae) contained substantial amounts of Glc*p*A lacking a methyl group (Fig. 2, Supplementary Fig. S1).

The ion distribution in most of the MALDI-TOF mass spectra is consistent with the products expected to be formed when a GX is fragmented with a family GH11 xylanase. However, the spectra of the xylo-oligosaccharides of several members of the Asparagales including
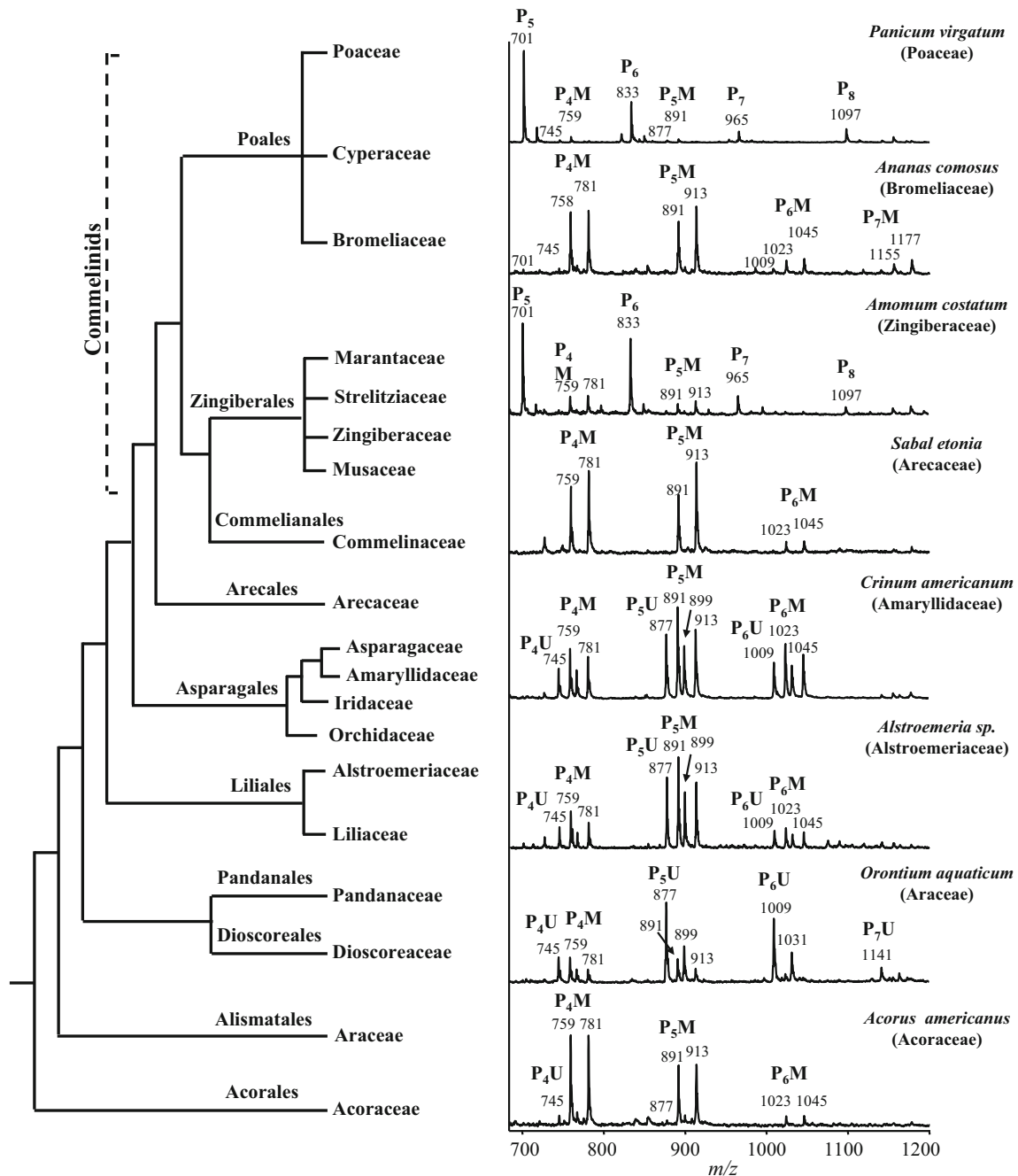
Fig. 2 MALDI-TOF mass spectra of the partially purified xylo-oligosaccharides generated by xylanase treatment of the 1 M KOH-soluble material from the cell walls of selected monocot genera to illustrate the structural diversity of xylans. The number of glycosyl residues in the xylo-oligosaccharides is indicated above the corresponding $[M + Na]^+$ and $[M - H + 2Na]^+$ ions in each spectrum. *P*, *M*, and *U* indicate pentose, methyl-GlcA, and GlcA, respectively. The monocot phylogenetic tree is adapted from Chase et al. (2006)

Ludisia discolor (Orchidaceae), *Crinum americanum* and *Clivia miniata* (Amaryllidaceae) did not conform to this distribution as they were enriched in ions that correspond to oligosaccharides composed of six pentoses and a uronic acid (Fig. 2, Supplementary Fig. S1). The spectrum of the *Clivia miniata* (Amaryllidaceae) xylo-oligosaccharides also indicates that this plant produces GX with a higher Me-GlcpA to GlcpA ratio than those produced by other Asparagales. The xylo-oligosaccharides from two Araceae (Alismatales), *Orontium aquaticum* (Fig. 2) and *Elodea canadensis* (Supplementary Fig. S1), also contained elevated amounts of oligosaccharides containing six pentoses and a uronic acid. Such oligosaccharides are typically generated by the family GH11 endoxylanase when acting

on xylans with side chains that contain pentosyl residues. To extend the results of these MS analyses, we used 1D and 2D NMR spectroscopy to gain further insight into the structures of the side chain substituents and diverse pentose-containing side chain structures generated from the commelinid and non-commelinid xylans.

NMR spectroscopy provides further insight into the structural features characteristic of commelinid and non-commelinid xylans

The 1D and 2D NMR spectroscopic analyses of the xylo-oligosaccharides allowed us to obtain information on the structures and relative abundances of the side chain substituents in the xylans from each monocot species examined.

Resonances characteristic of GlcpA substituents were observed in the ^{1}H-NMR spectra of the xylo-oligosaccharides generated from commelinid and non-commelinid monocot heteroxylans (Fig. 3, Supplementary Figs. S2–5). These GlcpA residues were typically 4-O-methylated. The extent of GlcpA methylation in xylans is known to differ depending on the species, the tissue, and the development stage. For example, virtually all of the GlcpA is 4-O-methylated in woody dicot GX, whereas in Arabidopsis GX the degree of 4-O-methylation varies from 40 to 70 % depending on the plant's developmental stage. None of the GlcpA is methylated in the GX of the moss *Physcomitrella patens* (Kulkarni et al. 2012b).

The GlcA residues in all the monocot xylans analyzed in this study were 4-O-methylated to some extent, with degrees of methylation that varied from 40 to 100 % (Table 1). GlcpA- and MeGlcpA-containing side chains were the only backbone substituents detected in GX from the non-commelinid monocots (Table 1). The xylans from all the commelinids analyzed also contained Araf substituents at O-3 of many of the backbone xylosyl residues. These Araf residues are the most abundant backbone substituent of the GAX in the Poaceae (Table 1; Fig. 3, Supplementary Fig. S2). We also detected resonances corresponding to Araf bearing a substituent at O-2 (i.e., 2-substituted Araf) in the spectra of all the Poales analyzed (Fig. 1a; Table 1; Supplementary Fig. S2), but not in the spectra of the other commelinids (Supplementary Fig. S3). Thus, 2-substituted Araf may be a unique characteristic of Poales GAX.

Our NMR and MALDI-TOF MS data are consistent with the notion that Araf substituents are one of the structural motifs that distinguishes commelinid xylans from their non-commelinid counterparts (Table 1). The Arecales, which are the basal commelinids, are comprised of only one family, the Arecaceae. The xylans of the Arecaceae (*Sabal etonia*, *Cocos nucifera,* and *Howea*

forsteriana) contain much more MeGlcpA than Araf (Fig. 3, Supplementary Fig. S3; Table 1). Thus, the Arecales produce xylans that have structural homology with non-commelinid GX including the presence of sequence **1** at the reducing end. We also detected **1** in all the Zingiberales and Commelinales xylans analyzed (Table 1, Supplementary Fig. S3). Previously, it was reported that **1** is absent in the GAX of the Poaceae (Poales) (Kulkarni et al. 2012a; Ratnayake et al. 2014). Our analysis indicates that **1** is also absent in the GAX of other Poales including *Cyperus alternifolius* (Cyperaceae) and *Tillandsia usneoides* (Bromeliaceae) (Table 1). Weak, but clearly discernible resonances diagnostic for the GalpA and Rhap residues of **1** were present in the ^{1}H-NMR spectrum of the xylo-oligosaccharides of *Ananas comosus* (pineapple, Bromeliaceae) (Table 1; Fig. 3). Thus, **1** was detected in at least one species of each order in the commelinid clade (Table 1). These results indicate that **1** is far more widespread among the monocots than we anticipated. Nevertheless, **1** was not detected in all monocot xylans. For example, no resonances characteristic of **1** were discernible in the NMR spectra of the xylo-oligosaccharides from several non-commelinid monocots (Table 1; Fig. 3, Supplementary Figs. S4 and S5), including *Spirodela polyrhiza* and *Lemna minor* (Araceae, Alismatales) and *Agapanthus africanus* and *Allium cepa* (Amaryllidaceae, Asparagales).

Structural characterization of the α-L-Arap-(1 → 2)-α-D-GlcpA-(1 → side chain of Alismatales and Asparagales Xylan

The 1D ^{1}H-NMR spectra of xylo-oligosaccharides generated from the xylan of several Asparagales and Alismatales species (Fig. 3, Supplementary Figs. S4 and S5) contain strong signals at δ 5.41. These signals are diagnostic for GlcpA or MeGlcpA residues bearing a substituent at O-2 (Shatalov et al. 1999; Togashi et al. 2009; Zhong et al. 2014). Signals at δ 5.41 may also originate from starch, which are often a contaminant of isolated cell walls. Nevertheless, our 2D NMR analysis established that these signals did not originate from starch-derived oligosaccharides.

To unambiguously identify the substituted GlcpA/MeGlcpA residues, we recorded high-resolution gCOSY spectra of the purified xylo-oligosaccharides from *Spirodela polyrhiza* (Alismatales, Fig. 4a) and *Crinum americanum* (Asparagales, Fig. 4b). Analysis of these gCOSY spectra allowed us to identify and assign the resonances of isolated spin systems with chemical shifts and coupling patterns characteristic of 2-substituted GlcpA for *Spirodela polyrhiza* (Fig. 4a) or 2-substituted GlcpA and MeGlcpA for *Crinum americanum* (Fig. 4b). The remaining ^{1}H and ^{13}C resonances of the xylo-oligosaccharide residues were
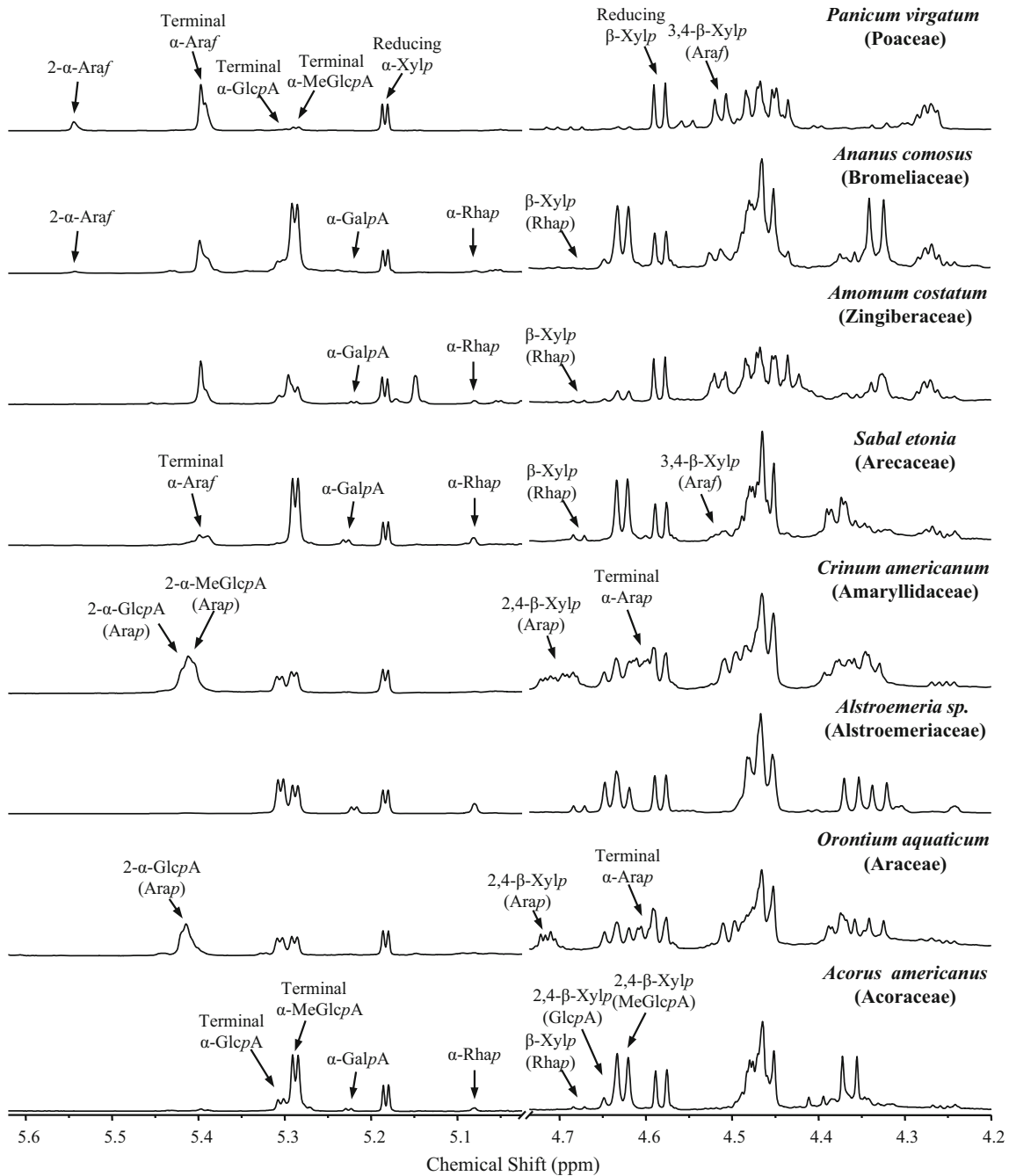
Fig. 3 Partial 600-MHz 1D ^{1}H NMR spectra of xylo-oligosaccharides generated as described in Fig. 2. The resonances diagnostic for the main structural features present in each monocot xylan are shown

assigned using homonuclear ROESY and heteronuclear (gHSQC and gHMBC) 2D NMR experiments (Table 2; Figs. 4, 5). These analyses established that the substituted GlcpA is attached to O-2 of a 4-linked Xylp. For example, in the Crinum americanum gHMBC spectrum, the cross-peak between C-1 (δ 97.3) of the 2-linked GlcpA and H-2 (δ 3.56) of the 2,4-linked Xylp confirmed that the GlcpA residue is linked to O-2 of the Xylp residue (Table 2; Fig. 5b).

The results of several studies have indicated that GlcpA is substituted at O-2 with a hexose (D-Galp) or with a partially characterized pentose in some dicots GXs (Shatalov et al. 1999; Togashi et al. 2009; Zhong et al. 2014; Chong et al. 2015; Mortimer et al. 2015). Our MALDI-TOF mass spectra (Fig. 2) are consistent with the presence of xylo-oligosaccharides containing an additional pentose as they contain a high abundance of ions corresponding to oligosaccharides with six pentoses and one uronic acid. No

Table 1 The major structural motifs of monocot xylans

Order (family)	Species	Seq. 1	Side chain					
			Terminal MeGlcA	Terminal GlcA	2-MeGlcA (Ara*p*)	2-GlcA (Ara*p*)	Terminal Ara*f*-(1 → 3)	2-linked Ara*f*
Commelinids			Relative abundance (%)					
Poales (Poaceae)	*Brachypodium distachyon*	ND	12	8	ND	ND	72	8
	Panicum virgatum	ND	9	2	ND	ND	75	14
	Oryza sativa	ND	9	9	ND	ND	69	13
	Miscanthus × giganteus	ND	14	1	ND	ND	73	12
	Setaria italica	ND	20	5	ND	ND	66	9
Poales (Cyperaceae)	*Cyperus alternifolius*	ND	43	6	ND	ND	45	6
Poales (Bromeliaceae)	*Ananas comosus*	tr	64	9	ND	ND	26	1
	Tillandsia usneoides	ND	46	1	ND	ND	44	8
Zingiberales (Zingiberaceae)	*Amomum costatum*	+	27	9	ND	ND	64	ND
	Hedychium coronarium	+	38	11	ND	ND	52	ND
Zingiberales (Strelitziaceae)	*Strelitzia alba*	+	52	31	ND	ND	17	ND
Commelinales (Commelinaceae)	*Tradescantia virginiana*	+	58	7	ND	ND	36	ND
Arecales (Arecaceae)	*Sabal etonia*	+	78	1	5	ND	16	ND
	Cocos nucifera	+	99	1	tr	ND	tr	ND
	Howea forsteriana	+	98	2	tr	ND	tr	ND
Non-Commelinids								
Asparagales (Amaryllidaceae)	*Crinum americanum*	tr	21	21	36	22	ND	ND
	Agapanthus africanus	ND	21	13	39	27	ND	ND
	Allium cepa	ND	37	3	35	25	ND	ND
Asparagales (Asparagaceae)	*Asparagus officinalis* (Tip)	tr	75	4	21	tr	ND	ND
	Asparagus officinalis (Stem)	+	90	10	tr	ND	ND	ND
	Agave americana	+	94	6	ND	ND	ND	ND
Liliales (Alstroemeriaceae)	*Alstroemeria* sp.	+	45	55	tr	tr	ND	ND
Liales (Liliaceae)	*Tulipa* sp.	+	94	16	ND	ND	ND	ND
Pandales (Pandanaceae)	*Pandanus utilis*	+	97	3	tr	ND	ND	ND
Dioscoreales (Dioscoreaceae)	*Dioscorea alata*	+	74	26	tr	ND	ND	ND
Alismatales (Araceae)	*Orontium aquaticum*	+	30	28	ND	42	ND	ND
	Spirodela polyrhiza	ND	22	22	ND	56	ND	ND
	Lemna minor	ND	100	ND	ND	ND	ND	ND
Acorales (Acoraceae)	*Acorus americanus*	+	85	15	ND	ND	ND	ND

ND not detected, *tr* trace amount (<1 %)

substantial ions corresponding to xylo-oligosaccharides containing a hexosyl residue were detected, suggesting that oligosaccharides containing galactose linked to Glc*p*A are of low abundance or completely absent in non-commelinid monocot GX.

β-D-Gal*p* and α-L-Ara*p* residues are structural homologs that are difficult to distinguish by ^{1}H NMR spectroscopy but can be differentiated by ^{13}C NMR spectroscopy. Indeed, the ^{13}C NMR spectra of the *Spirodela polyrhiza* and *Crinum americanum* xylo-oligosaccharides contain signals with chemical shifts for C-1 (δ 105.2) and C-5 (δ

67.1) that are diagnostic of Ara*p* residues (Table 2; Figs. 4, 5a) (Glushka et al. 2003; Peña et al. 2008). The gHMBC spectrum (Fig. 5b) contains a cross-peak between C-1 (δ 105.2) of the Ara*p* residue and H-2 (δ 3.77) of the 2-linked Glc*p*A residue that shows that the Ara*p* is attached to O-2 of the Glc*p*A. The presence of this α-L-Ara*p*-(1 → 2)-α-D-Glc*p*A-(1 → side chain is consistent with our MALDI analysis of the xylan from selected Asparagales and Alismatales.

Further NMR analysis established that *Crinum americanum* xylan contains the structurally related side chain α-
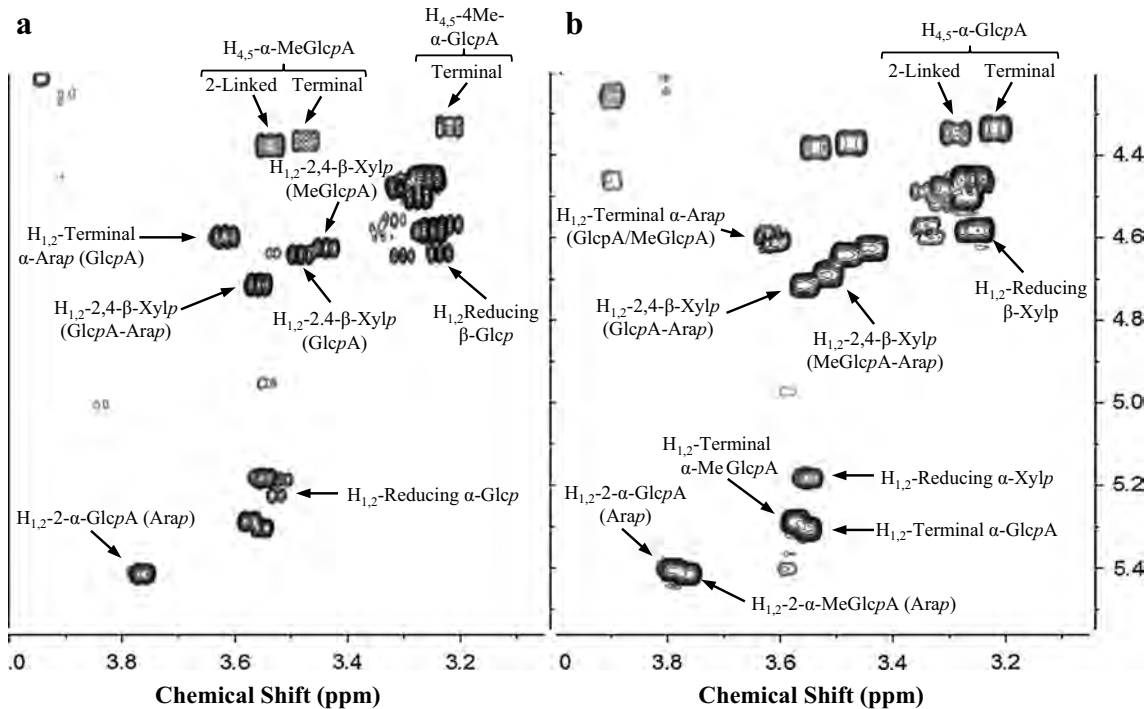
Fig. 4 Partial 600-MHz high-resolution gCOSY spectra of the xylo-oligosaccharides generated from *Spirodela* and *Crinum*. **a** *Spirodela polyrhiza* (Araceae, Alismatales) and **b** *Crinum americanum* (Amaryllidaceae, Asparagales) xylans. The labeled cross-peaks correspond to the correlations between vicinal protons of the glycosyl residues in the oligosaccharide side chains. For example, $H_{1,2}$-2,4-β-Xylp (GlcpA-Arap) corresponds to the correlation between the H_1 and H_2 of a 4-linked β-Xylp substituted at *O*-2 with a GlcA that is itself substituted at *O*-2 with an α-L-Arap residue (see Fig. 1 for oligosaccharide structures)

Table 2 ^1H and ^{13}C NMR assignments for the side chains containing GlcA/MeGlcA substituted with α-L-Arap residues present in Asparagales, Alismatales, and *Eucalyptus grandis* GX

Residue	H1/C1[a]	H2/C2	H3/C3	H4/C4	H5/C5	H6/C6
-(1 → 4)-[α-L-Arap-(1 → 2)-α-D-GlcpA-(1 → 2)]-α-D-Xylp-(1 → 4)-						
α-L-Arap	4.60/105.4	3.62/71.6	3.68/72	3.94/69	3.93–3.67/67.2	
2-α-D-GlcpA	5.42/97.3	3.76/79.3	3.94/72.4	3.53/72.4	4.38/72.5	
2,4-β-D-Xylp	4.71/101.2	3.55/76.2	3.69/72.4	3.81/77.0	4.13–3.44/63.1	
-(1 → 4)-[α-L-Arap-(1 → 2)-4-*O*-methyl-α-D-GlcpA-(1 → 2)]-α-D-Xylp-(1 → 4)-						
α-L-Arap	4.61/105.3	3.61/71.7	3.68/73	3.94/69	3.93–3.67/67.2	
2-α-D-GlcpA	5.41/97.1	3.79/79.3	3.97/72.2	3.29/82.9	4.35/72	
2,4-β-D-Xylp	4.69/101.3	3.51/76.1	3.66/72.6	3.81/77.0	4.10–3.43/63	
-(1 → 4)-[β-D-Galp-(1 → 2)-4-*O*-methyl-α-D-GlcpA-(1 → 2)]-α-D-Xylp-(1 → 4)-						
β-D-Galp	4.70/104.7	3.58/72	3.67/73	3.93/69	3.7/	3.8-3.8/61.7
2-α-D-GlcpA	5.43/97.1	3.88/78.4	3.98/72.5	3.29/82.9	4.39/72	
2,4-β-D-Xylp	4.67/101.6	3.51/76	3.66/72	3.80/77	4.10–3.40/63	

The corresponding assignments for the β-D-Galp-(1 → 2)-MeGlcpA side chain in *Eucalyptus* GX are also shown

[a] Chemical shifts are reported in ppm relative to internal acetone, δ_H 2.225 and δ_C 30.89

L-Arap-(1 → 2)-4-*O*-Me-α-D-GlcpA-(1 → 2)- (Table 2; Figs. 4, 5). This disaccharide is the most abundant side chain in the xylan from several Asparagales species, including *Crinum americanum*, *Agapanthus africanus*, *Clivia miniata*, *Allium cepa* (Amaryllidaceae), and *Ludisia discolor* (Orchidaceae) and in the Alismatales, *Spirodela polyrhiza*, *Orontium aquaticum*, and *Elodea canadensis*

(Table 1; Fig. 2, Supplementary Figs. S4 and S5). Weak signals that are diagnostic for an α-L-Arap-containing acidic side chain were also detected in the ^1H-NMR spectra of xylo-oligosaccharides of numerous other monocots (see Table 1).

The xylo-oligosaccharides generated from *Eucalyptus globulus* wood GX have been shown to contain a β-Galp-
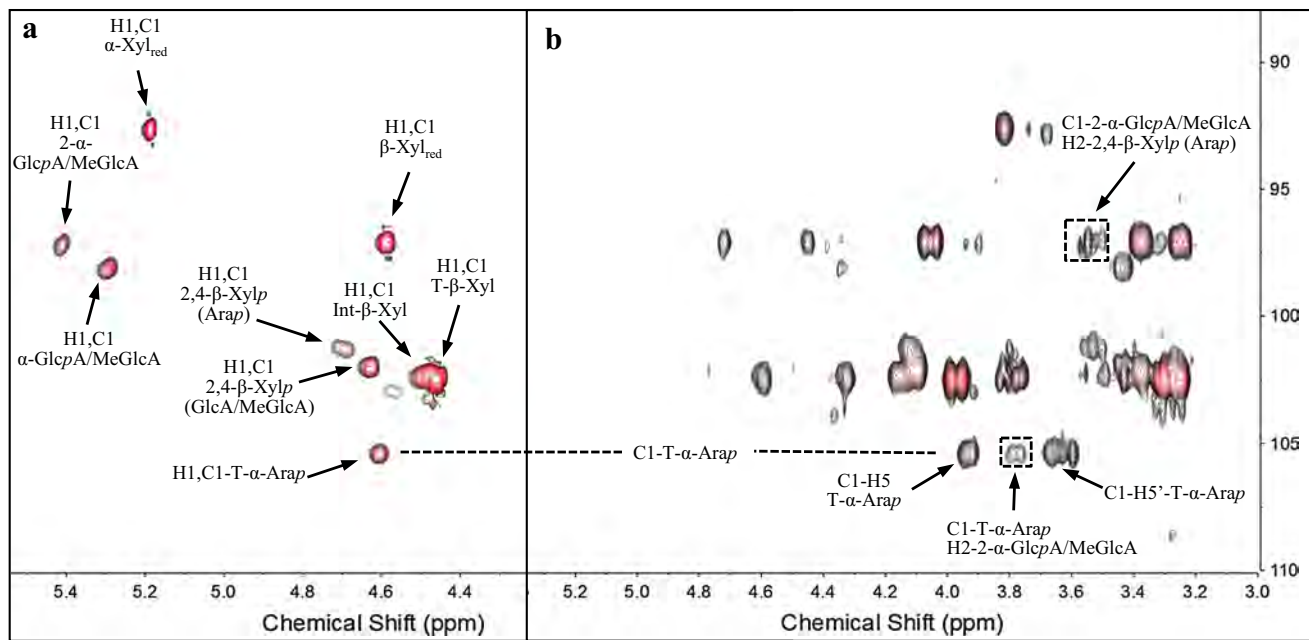
Fig. 5 Partial 600-MHz heteronuclear NMR spectra of xylo-oligosaccharides isolated from *Crinum americanum* (Amaryllidaceae, Asparagales). **a** gHSQC spectrum containing cross-peaks that correspond to one-bond correlation between the ^{1}H and ^{13}C. Diagnostic signals for the Ara*p*-containing side chain are labeled. **b** Interglycosidic cross-peaks (in *squares*) in the gHMBC spectrum establish that the α-L-Ara*p* is linked to *O*-2 of the GlcA/MeGlcA that is itself linked to *O*-2 of an internal 4-linked Xyl residue. *T* terminal, *int* internal, *red* reducing residues

(1 → 2)-4-*O*-methyl-α-Glc*p*A-(1 → 2)- side chain (Togashi et al. 2009). Thus, we next determined using NMR if *Eucalyptus* xylan also has Ara*p* linked to Glc*p*A. Resonances diagnostic for both the β-Gal*p* (1 → 2)-4-*O*-methyl-α-Glc*p*A-(1 → 2) and the α-L-Ara*p*-(1 → 2)-α-D-Glc*p*A-(1 → 2)- side chains are present in the gCOSY spectra of *Eucalyptus grandis* xylo-oligosaccharides (Supplementary Fig. S6). Together, these data show that GX containing the Ara*p*-GlcA side chain is a common feature of non-commelinid monocots and provide further evidence that it is present in dicot GX (Chong et al. 2015; Mortimer et al. 2015).

Xylan structure shows organ-specific variations in selected monocots genera

The cell wall xylans of commelinids, other than the Poales, have structural features that are comparable to the GAX of Poaceae walls (single Ara*f* side chains) and to the GX of eudicot secondary walls (high abundance of MeGlc*p*A and Glc*p*A and presence of sequence **1**) (see Table 1). To determine whether these different structural features are predominantly associated with primary or with secondary wall xylans, the xylans isolated from leaves and stems of *Tradescantia virginiata* (family Commelinaceae, Commelinales) were structurally characterized. Acidic xylo-oligosaccharides that are characteristic of GX in eudicot

secondary walls were predominant in the MALDI-TOF MS of the stem xylo-oligosaccharides (Fig. 6a). By contrast, neutral xylo-oligosaccharides were more abundant in leaves, which are rich in primary walls. Thus, the *Tradescantia virginiata* leaf xylan is comparable with the Poaceae GAX where neutral Ara*f*-containing substituents predominate.

In a second series of experiments, we found that the xylans isolated from *Asparagus officinalis* organs enriched in either primary or secondary walls are also structurally distinct. For example, the GX from growing tips of shoots contains the Ara*p*-(1,2)-Glc*p*A-(1, side chain but only trace amounts of **1** were discernible. The stem and "leaf" GXs had features characteristic of eudicot secondary wall GX, including the presence of sequence **1** at the reducing end (Fig. 6b). Although this result at first sight was surprising, it is consistent with the fact that in *Asparagus* what appear to be the leaves are in fact modified stems (cladodes or phylloclades); the true leaves are scale-like structures on the stem.

The reducing end xylose of Poaceae secondary wall xylan is often substituted at *O*-2 with MeGlcA or at *O*-3 with Ara*f*

Our results and previous studies have shown that GAX isolated from secondary cell walls of Poaceae lacks

a

Tradescantia virginiata (Commelinaceae)

b

*Asparagus officinalis (*Asparagaceae)
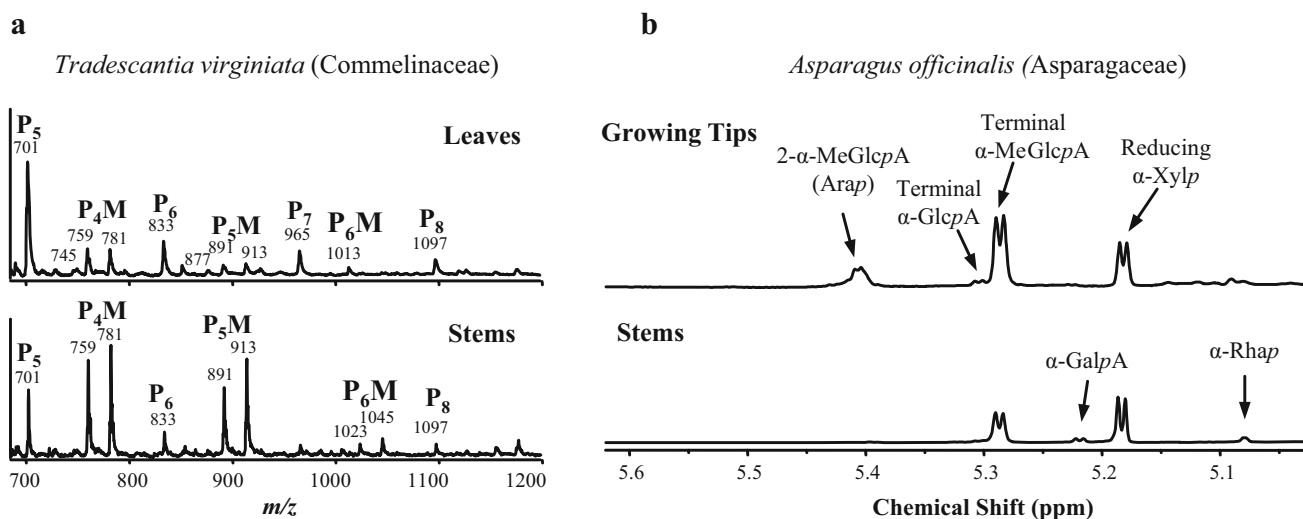
Fig. 6 Structural differences in xylo-oligosaccharides obtained from different organs of the same plant. **a** MALDI-TOF mass spectra of xylo-oligosaccharides obtain from leaves (*top*) and stem (*bottom*) of

Tradescantia virginiata. **b** Partial 600-MHz 1D NMR spectra of xylo-oligosaccharides partially purified from *Asparagus officinalis* growing tips of shoots and stems of mature plants

discernible amounts of **1** at their reducing end (Kulkarni et al. 2012a). Ratnayake and colleagues reported that the reducing end xylose of *Triticum aestivum* (wheat) endosperm GAX is often substituted at *O*-3 with an α-L-Ara*f* residue or at *O*-2 with an α-D-Glc*p*A residue (Ratnayake et al. 2014). To extend these studies and to identify the glycosyl sequence at the reducing end of the GAX in the secondary cell walls of Poaceae, we used the following approach. The AIRs of the five Poaceae were treated with 2AB in the presence of sodium cyanoborohydride. This reductive amination procedure converts any exposed reducing end glycose to its corresponding 2AB-labeled derivative. The GAX was then solubilized from the AIR and fragmented with endoxylanase. Xylo-oligosaccharides containing xylitol-2AB correspond to the sequence of glycoses that were located at the reducing end of the intact polysaccharide. The 2AB-labeled xylo-oligosaccharides were purified and separated into neutral and acidic fractions using a combination of SEC and solid-phase extraction with graphitized carbon and then structurally characterized using MALDI-TOF MS, ESI MS[n], and 1D and 2D NMR spectroscopy.

Complete chemical shift assignments of the glycosyl residues comprising the most abundant components of the mixture of 2AB-labeled acidic xylo-oligosaccharides of *Setaria italica* (foxtail millet) were obtained using 1D and 2D (TOCSY, HSQC, ROESY, HMBC) NMR experiments (Fig. 7; Table 3). The predominant 2AB-labeled oligoglycosyl alditol contained one MeGlc*p*A residue, two xylosyl residues, and a 2AB-derivatized xylitol. The chemical shift values for 2AB-labeled xylitol are, with the exception of the C-2 resonance, consistent with previously published
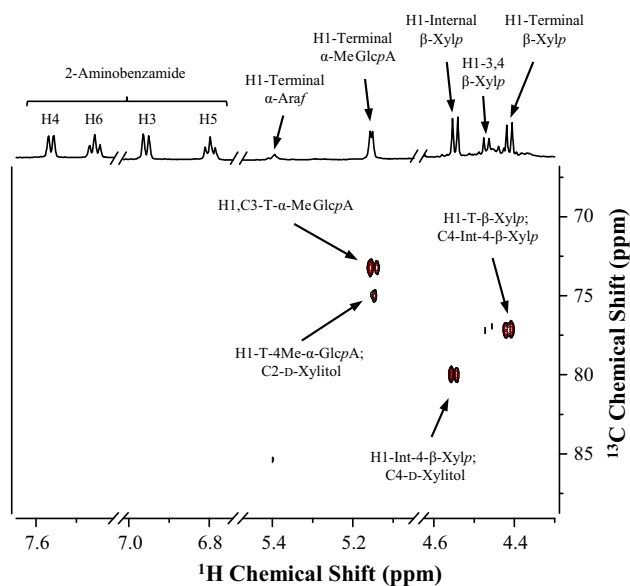
Fig. 7 NMR analysis of the 2AB-labeled acidic xylo-oligosaccharides generated by endoxylanase treatment of the 1 M KOH-soluble material from 2AB-labeled *Setaria italica* AIR. *Top* the 1D ¹H NMR spectrum contains resonances of comparable intensity for 2AB, terminal MeGlcA, terminal and internal xylose indicating the predominant oligosaccharide is composed of these residues. *Bottom* the interglycosidic cross-peaks in the gHMBC spectrum establish that the MeGlcA residue is linked to *O*-2 of the 2AB-labeled xylitol and that the structure of the predominant oligosaccharide is Xyl-Xyl-(MeGlcA)-xylitol-2AB. The presence of 2AB-labeled xylitol shows that the oligosaccharide was present at the reducing end of the GAX

data (Ishii et al. 2008). The downfield shift of this resonance indicates the presence of a substituent at *O*-2. Indeed, the gHMBC spectrum contained a cross-peak between H-1 of the terminal MeGlc*p*A and the C-2 of the

Table 3 ^{1}H and ^{13}C NMR assignments of the 2AB-labeled acidic xylo-oligosaccharides obtained by endoxylanase treatment of the 1 M KOH-soluble material from the 2AB-labeled AIR of the Poaceae

Residue	H1/C1 Chemical shift (ppm)[a]	H2/C2	H3/C3	H4/C4	H5/C5
β-Xylp (terminal)[b]	4.41/102.5	3.25/73.6	3.44/76.2	3.63/69.9	3.98–3.32/66.0
β-1,4-Xylp (internal)	4.55/102.7	3.27/73.55	3.53/74.3	3.68/77.1	3.95–3.30/63.5
D-Xylitol [Xyl-2AB]	3.57/42.5	4.09/75.1	4.00/70.6	3.95/79.9	3.84–3.74/61.0
α-4Me-GlcpA	5.15/97.4	3.60/72.0	3.77/73.0	3.24/82.9	4.04/73.1
β-Xylp (terminal)[c]	4.47/102.9	3.27/73.6	3.42/76.2	3.60/69.9	3.97–3.30/66.0
β-Xylp (internal)[c]	4.43/102.5	3.28	3.43	3.79	4.12–3.39/63.6
β-1,3,4-Xylp (α-L-Araf)[c]	4.48/102.7	3.40	3.7		
α-L-Araf (terminal)[c]	5.39/108.2	4.16/72.0	3.90/78.0	4.27/85.6	3.79–3.72/61.7

[a] Chemical shifts are reported in ppm relative to internal acetone, δ_H 2.225 and δ_C 30.89. Signals for xylitol are actually for xylitol that has 2AB and an α-4Me-GlcpA attached to it

[b] The most abundant xylo-oligosaccharide is Xyl-Xyl-(GlcA)Xyl-2AB

[c] Low-abundance resonances consistent with the presence of other oligosaccharides, including Xyl-Xyl-Xyl-(GlcA)Xyl-2AB and Xyl-(Ara)Xyl-(GlcA)-Xyl-2AB, in the mixture

2AB-xylitol showing that a MeGlcpA residue is linked to O-2 of the xylitol (Fig. 7; Table 3). The gHMBC spectrum also contained a cross-peak correlating H-1 of an internal 4-linked β-D-Xylp residue with C-4 of the xylitol-2AB residue, indicating that this β-D-Xylp residue is linked to O-4 of the xylitol AB. Finally, a cross-peak correlated H-1 of a terminal β-D-Xylp residue with C-4 of the internal 4-linked β-D-Xylp residue, which itself is linked to O-4 of the xylitol-2AB residue (Fig. 7; Table 3). These results together show that the predominant oligosaccharide in the mixture is β-D-Xylp-(1 → 4)-β-D-Xylp–(1 → 4)-[MeGlcA-(1 → 2)-]-xylitol-2AB (Fig. 1b). Other weaker resonances observed in the 2D spectra indicate that small amounts of Xyl-(Ara)-Xyl-(MeGlcA)-Xyl-2AB and Xyl-Xyl-Xyl-(MeGlcA)-Xyl-2AB were also present in the *Setaria italica* GAX. Thus, the reducing end xylose residue of this GAX is frequently substituted at O-2 with a MeGlcpA residue.

Our NMR analysis of the 2AB-labeled neutral xylo-oligosaccharides from *Setaria italica* indicated a high abundance of Araf side chains, but the mixture was too complex to be fully characterized by this technique. Thus, the neutral and acidic 2AB-labeled xylo-oligosaccharides were per-O-methylated and analyzed by ESI MS^n. The ESI MS^n spectra of these oligosaccharides are dominated by Y and B ions, which provide extensive sequence information (Domon and Costello 1988; Mazumder and York 2010). Y ions, which correspond to fragments generated by loss of residues from the non-reducing end, were abundant due to the presence of the 2AB-labeled xylitol at the former reducing end of the oligosaccharides. B ions are fragments generated by loss of residues from the reducing terminus and were much less abundant in the ESI spectra.

The full-scan ESI mass spectrum of the per-O-methylated acidic oligosaccharides from *Setaria italica* contained a series of [M + Na]$^+$ ions at m/z 769, 929, 1089, 1249, which correspond to 2AB-labeled oligosaccharides containing a 2AB-labeled xylitol, one to four pentosyl residues, and a single uronic acid (Supplementary Fig. S7a). Based on our NMR analysis, the uronic acid is almost always MeGlcA. The parallel series of ions at 14 Da lower mass likely corresponds to oligosaccharides lacking one O-methyl substituent and may result from incomplete methylation of the 2AB moiety. The fully methylated precursor ions at m/z 929 and 1089 were selected for MS fragmentation studies.

The quasimolecular ion at m/z 929 in this spectrum corresponds to a methylated 2AB-labeled oligosaccharide composed of a 2AB-labeled xylitol, two pentoses, and one uronic acid. The ESI MS^2 and MS^3 spectra (Fig. S8) contained a fragment ions series 929-755-595/523 that, together with NMR analysis and the mode of action of the family GH11 xylanase used to fragment the xylan, establish that the structure of this oligosaccharide is Xyl-Xyl-(MeGlcA)-Xyl-2AB.

The quasimolecular ion at m/z 1089 in the ESI spectrum of the per-O-methylated 2AB-labeled, acidic, xylo-oligosaccharides from *Setaria italica* corresponds to an oligosaccharide composed of a 2AB-labeled xylitol, three pentosyl residues, and one GlcpA, which is 4-O-methylated in the native structure. ESI MS^n here indicated the existence of two or more distinct oligosaccharides (Supplementary Fig. S9). For example, the series of fragment ions at m/z 1089-915-755-595/523 is consistent with the sequence Xyl-Xyl-Xyl-(GlcA)-Xyl-2AB, whereas the series of fragment ions at m/z 1089-915-741-595 provides evidence that sequence Xyl-(Pentosyl)-Xyl-(GlcA)-Xyl-2AB is present, where the pentosyl residue is most likely Araf based on our NMR data.

The ESI mass spectrum of the fraction enriched in the methylated neutral 2AB-labeled oligosaccharides (obtained by elution of the SPE cartridge with 25 % acetonitrile)

gave a series of $[M + Na]^+$ ions at *m/z* 711, 871, 1031, and 1191 (Supplementary Fig. S7b), corresponding to oligosaccharides containing between 2 and 5 xyloses and a 2AB-xylitol. ESI MS^n of the ion at *m/z* 1031 indicated that this ion can arise from both a linear and a branched sequence (Fig. 8). For example, the fragmentation pathways *m/z* 1031-857-683-537-363 and 1031-857-697-537-363 establish the presence of a pentosyl residue linked to the 2AB-xylitol residue Fig. 8). However, the fragmentation pathway at *m/z* 1031-857-697-377 corresponded to a linear oligosaccharide, i.e., Xyl-Xyl-Xyl-Xyl-Xyl-2AB, thus indicating the presence of oligosaccharides in which the reducing end xylose is not branched.

Our combined ESI MS and NMR data provide substantial evidence that most but not all of the xylose at the reducing end of the GAX isolated from *Setaria italica* secondary walls is branched. Comparable results were obtained with the 2AB-labeled xylo-oligosaccharides generated from the 2AB-treated AIR of *Miscanthus x giganteus*, *Panicum virgatum*, *Oryza sativa*, and *Brachypodium distachyon*. Thus, in all of the Poaceae GAXs examined, the predominant reducing end structure is a xylose substituted either at *O*-2 with 4-*O*-MeGlc*p*A or at *O*-3 with Ara*f* residue (Figs. 7, 8, Supplementary Figs. S7–S9). The presence of a 4-*O*-MeGlc*p*A substituent rather than a Glc*p*A substituent on the reducing end xylose of secondary wall GXs is one structural feature that distinguishes them from their wheat endosperm counterparts (Ratnayake et al. 2014).

Discussion

Monocot xylans are more structurally diverse than was previously reported

Our structural characterization of cell wall xylans from genera of 10 of the 12 monocot orders provides a new perspective on the diversity, function, and evolution of monocot cell walls. For example, the xylans from many Alismatales and Asparagales lack sequence **1** and their most abundant backbone substituents are disaccharides consisting of MeGlc*p*A or Glc*p*A with an Ara*p* substituent at *O*-2 (Tables 1, 2; Figs. 1, 4, 5). These disaccharides are widespread among non-commelinid xylans but are present only in trace amounts in Arecales xylan and were not detected in the GAXs of the more derived commelinids (Table 1).

Side chains containing a substituted MeGlc*p*A were first identified in *Eucalyptus* GX (Shatalov et al. 1999; Reis et al. 2005). Detailed analyses of the xylo-oligosaccharides generated from *Eucalyptus globulus* wood GX established that one of these side chains is β-Gal*p*-(1 → 2)-4-*O*-methyl-α-Glc*p*A-(1 → 2)- (Togashi et al. 2009). Glc*p*A

substituted with an incompletely characterized pentosyl residue has been detected in the GX isolated from *Arabidopsis thaliana* inflorescence stems (Chong et al. 2015). Mortimer et al. (2015) have tentatively identified the pentose as Ara*p* and suggested that the disaccharide is a component of a xylan present in the *Arabidopsis thaliana* primary wall. Our data unambiguously demonstrate that, in monocots and also in *Eucalyptus*, the pentose in this disaccharide side chain is α-L-Ara*p*. To date, only the GX isolated from the secondary cell walls of *Eucalyptus grandis* has both β-Gal*p*-(1 → 2)-MeGlc*p*A and α-L-Ara*p*-(1 → 2)-MeGlc*p*A side chains, which are structurally homologous. The role of these disaccharides in xylan function(s) is not known. Further studies are also required to determine the functional consequences of this structural diversity.

Our data suggest that the Ara*p*-containing GX we isolated from non-commelinid monocots is structurally similar to the primary wall GX described by Mortimer et al. (2015). Our results with *Asparagus officinalis* (Fig. 6b) also show that the Ara*p*-containing GX is most abundant in actively growing organs, which are rich in cells surrounded by a primary wall. Nevertheless, the presence of this side chain is not a fundamental feature of non-commelinid monocot primary wall GX as it was not detected in the GX isolated from *Lemna minor* cell walls (Table 1). *Lemna minor*, which is an aquatic plant, is composed predominantly of growing cells surrounded by primary walls and contains a very limited vascular system (Landolt 1986). Additional studies are required to determine whether the distribution of Ara*p*-containing GX is cell or tissue specific and to determine the functions of primary wall xylan.

Changes in xylan structure during the evolution and diversification of monocots

The combined results of numerous studies have shown that the primary walls of the graminids (clade in the Poales, commelinid monocots) are xylan rich and thus distinct from the pectin- and xyloglucan-rich primary walls of eudicots, non-commelinid monocots, and the Arecales (a basal non-graminid commelinid) (Harris and Hartley 1980; Bacic et al. 1988; Carpita and Gibeaut 1993; Carpita 1996; Harris et al. 1997). By contrast, the commelinids Zingiberales and Commelinales, which are more derived than the Arecales, have primary walls that contain similar proportions of pectin and hemicellulose (Harris et al. 1997; Harris 2006; Harris and Trethewey 2010). Our study extends the notion that wall composition varies according to commelinid phylogeny by showing that evolution and diversification within this clade were accompanied by pronounced changes in xylan structure, most notably by the appearance of Ara*f*-containing side chains and subsequent increase in
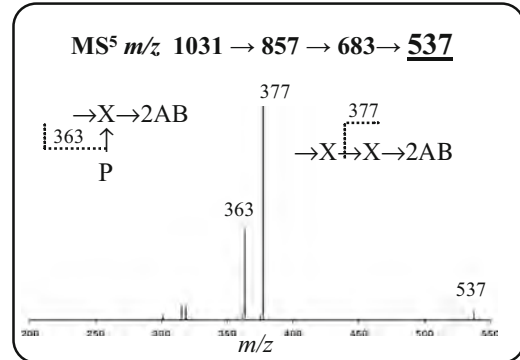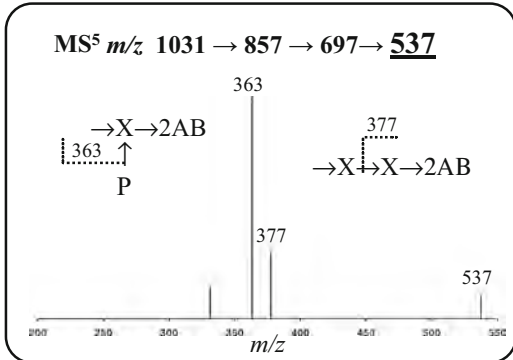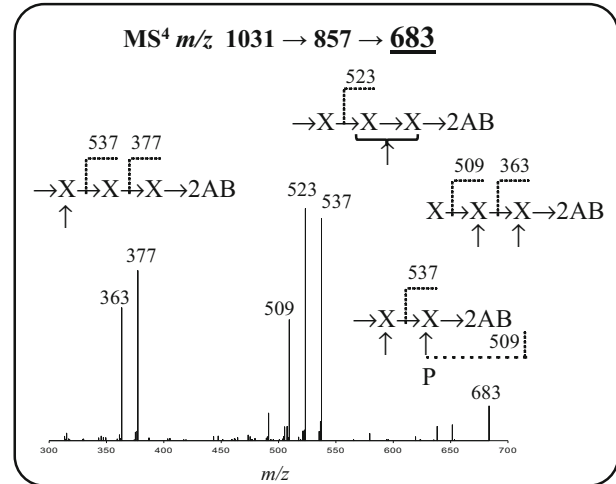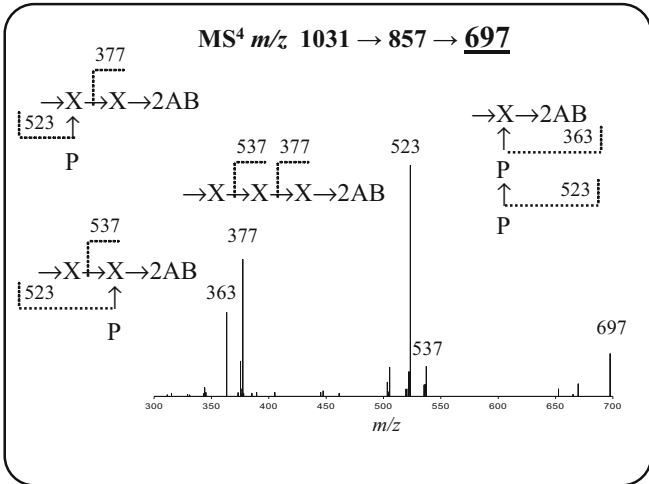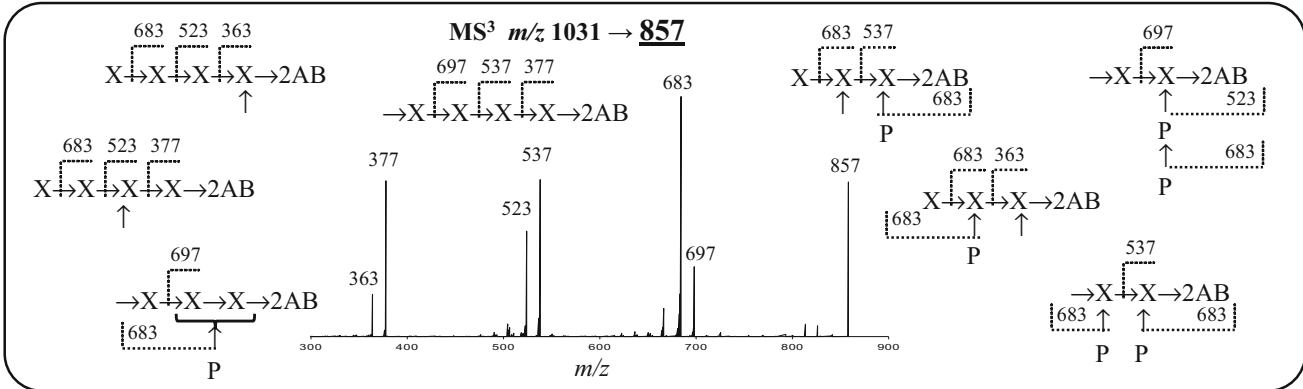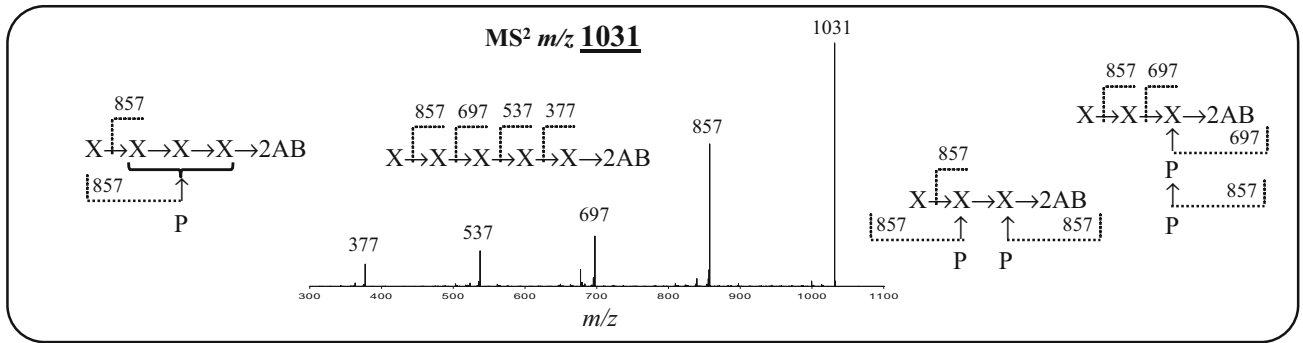
◄Fig. 8 ESI MS^n of the per-*O*-methylated and 2AB-labeled neutral xylo-oligosaccharide generated from *Setaria italica*. The *m/z* values for ions in the fragmentation pathway leading to the precursor ion for each MS^n spectrum are shown above the spectrum, and the *m/z* value for the immediate precursor ion is underlined. Several of the possible structures corresponding to each selected precursor ion are illustrated in the *box* containing the corresponding MS^n spectrum. Fragmentation of each of these precursor ions, leading to ions observed in the MS^n spectrum, is also illustrated. The most abundant fragment ions generated were Y ions, which contain the 2AB moiety. These data indicate that the initially selected precursor ion at *m/z* 1031 corresponds to several structurally distinct xylo-oligosaccharides and that the xylose at the reducing end of the oligosaccharides often bears a monoglycosyl or diglycosyl substituent. The same structures are present in the GAX isolated from *Miscanthus giganteus*, *Panicum virgatum*, *Oryza sativa*, and *Brachypodium distachyon*

the abundance of Ara*f*-containing xylan in their primary and secondary cell walls (see Table 1).

The Poales (Poaceae, Cyperaceae, and Bromeliaceae) are the most derived commelinids and produce GAX that contain side chains with terminal and 2-linked Ara*f* residues and little if any sequence **1**. However, Poaceae GAX contains relatively low levels of Glc*p*A and MeGlc*p*A and is thus distinct from Cyperaceae and Bromeliaceae GAX. No sequence **1** was detected in the Poaceae GAX; nevertheless, we cannot preclude the possibility that a small number of cells in these plants produce a xylan containing this sequence as trace amounts of **1** were detected in the xylan from *Ananas cosmosus* (Bromeliaceae) walls.

Ara*f*-containing side chains predominate in Poaceae GAX but account for only half of the backbone glycosyl substituents in the Cyperaceae and Bromeliaceae. Xylans in all the Zingiberales and Commelinales analyzed also contain similar proportions of Ara*f*- and Glc*p*A-/MeGlc*p*A-containing side chains, but were shown unambiguously to contain sequence **1** and lack side chains with 2-linked Ara*f*. The abundance of Ara*f* side chains is reduced to its lowest level in the GAX of the Arecales and results in a xylan with structural features that are more in common with the GXs of the non-commelinid monocots. We suggest that, among extant plants, the Arecales most closely resemble the ancestral monocots that first synthesized GAX. Such an observation is consistent with phylogenetic studies showing that the Arecales are the least derived commelinid (Carnachan and Harris 2000; Chase et al. 2006; Smith and Donoghue 2008).

Glycosyl sequence **1** is located at the reducing end of many but not all of the xylans produced by monocots (Table 1). The presence or absence of this sequence occurs both within and between orders and thus is unlikely to be directly correlated with the appearance of new orders during monocot evolution. Sequence **1** was readily identified in the GX isolated from *Asparagus officinalis* stems,

yet little if any of this sequence was detected in the GX isolated from growing tips of the shoots (Fig. 6; Table 1). Similarly, this sequence was not detected in the GXs isolated from the cell walls of two different duckweeds (Araceae), *Spirodela polyrhiza* and *Lemna minor* (see Table 1). These aquatic plants are composed predominantly of growing cells and contain very little vascular tissue (Landolt 1986). Thus, the presence of sequence **1** is likely to be a characteristic of the secondary cell wall xylans of many monocots. Notable exceptions are the GAXs in the secondary cell walls of Poales (Poaceae, Cyperaceae, and Bromeliaceae). These GAXs lack sequence **1** but often contain substituted xylosyl residues at their reducing end (Figs. 7, 8, Supplementary Figs. S7, S8, and S9). This structural feature was also identified in the primary wall GAX of *Triticum aestivum* endosperm (Ratnayake et al. 2014). It is not known whether the substituted reducing end xyloses are also present in the GXs of the Alismatales and Asparagales that also lack sequence **1**. Additional studies are required to identify the genes and enzymes involved in the biosynthesis of these reducing end sequences and to determine the relationship between the xylan's reducing end structure and its function in the cell wall.

Do non-graminid commelinids synthesize distinct GAXs and GXs?

We have shown that the Zingiberales and Commelinales analyzed in this study produce xylans with structural features characteristic of both graminid GAX and non-commelinid/dicot GX (Table 1). Most studies, including ours, have determined the structural characteristics of xylans by characterizing the oligosaccharides generated by endoxylanase fragmentation. This procedure cannot readily distinguish between the presence of two distinct polysaccharides that contain different structural motifs or a single polysaccharide that contains all the structural motifs. Nevertheless, we believe our results are more consistent with the presence of both GAX and GX as separate polysaccharides. For example, Ara*f* substituents are abundant in the xylan from the leaves of *Tradescantia virginiana* (Commelinaceae), whereas Glc*p*A/MeGlc*p*A substituents predominate in the stem xylan (Fig. 6). Such results are consistent with the predominance of GAX in leaf primary walls and GX in stem secondary walls. The presence of these two types of xylans in different organs of the plant may result from cell- and/or tissue-specific differences in the polysaccharide synthesis machinery as proposed for primary and secondary wall synthesis in Arabidopsis (Mortimer et al. 2015).

The cell walls of many Commelinales and Zingiberales contain xyloglucan that has characteristics of both eudicots

(XXXG type) and grasses (XXGn type) (Hsieh and Harris 2009). XXXG- and XXGn-type xyloglucans are also present in comparable proportions in the walls of the Bromeliaceae (Poales). It is not known whether one xyloglucan contains both structural motifs or whether distinct XXXG- and XXGn-type xyloglucans are formed by specific cells and/or tissues in the plant organs. This latter notion is not unprecedented as several examples of cell and tissue-specific differences in hemicellulose structure have been described. For example, the root hair walls of numerous plants including *Arabidopsis thaliana* and *Oryza sativa* (Peña et al. 2012; Liu et al. 2015), and *Nicotiana alata* pollen tube walls (Lampugnani et al. 2013) contain a xyloglucan, which is structurally distinct from the xyloglucan present in other tissues of the same plant. GX in the interfascicular fibers of *Arabidopsis thaliana* stems contains Glc*p*A and MeGlc*p*A substituents, whereas the Glc*p*A is fully methylated in the GX in stem and root vessels (Urbanowicz et al. 2012).

Our results suggest that organ-, tissue-, and cell-specific structural differences of the cell wall polysaccharides may be more substantial than the differences between taxonomic groups. This notion adds an additional layer of complexity to the study of cell wall diversity and evolution and is especially relevant in studies that infer the activities of gene products by the inability to detect a particular polysaccharide structure. Structurally distinct polysaccharide may indeed be synthesized by a limited number of specific cell types.

Origins of the graminid GAXs

The evolution and diversification of the commelinids were accompanied by substantial changes in the polysaccharide composition of the cell wall together with changes in the fine structures of the wall polysaccharides. Our results suggest that some of the changes in xylan structure are not necessarily species specific, since we found structural features characteristic of different types of xylan in the same species (Fig. 6; Table 1). We propose that one pivotal event involved the addition of Ara*f* residues to GX to form a prototypical GAX in a basal commelinid. This may have first occurred in cells that only produce primary walls but was then attained by cells producing secondary walls. This hypothesis is consistent with our results showing that the amount of Ara*f*-containing xylans increases through the commelinids and that these GAXs are the most abundant xylan in the Poaceae, which are the most derived monocots. The addition of Ara*f* residues may have endowed the newly formed GAX with physical properties that allowed it to perform some of the functions previously performed by xyloglucan and/or pectin, as previously suggested (Carpita 1996). Subsequently, the transition to primary cell walls

with decreased amounts of pectin and xyloglucan may have been facilitated by the ability to synthesize xylan with Ara*f* side chains.

In summary, we have shown that several structural motifs of xylan have changed during monocot evolution. Such data will be of value in studies to determine whether this structural diversity is reflected in changes in the molecular and cellular mechanisms that control the synthesis of these polysaccharides. Knowledge of differences in xylan structure will also facilitate the use of biomass from diverse monocots for conversion to biofuel and thereby contribute to sustainable biomass production.

Author contribution statement WSY, MJP, and MAO conceived and designed research. AK, JB, MAO, WSY, and MJP carried out experiments and analyzed the data. M. B. identified and provided plant materials. MJP, MAO, AK, and WSY wrote the manuscript. All authors read and approved the manuscript.

Compliance with ethical standards

Conflict of interest The authors declare that they have no conflict of interest

References

Bacic A, Harris P, Stone B (1988) Structure and function of plant cell walls. In: Preiss J (ed) The biochemistry of plants. Academic Press, San Diego, pp 297–371

Bigge J, Patel T, Bruce J, Goulding P, Charles S, Parekh R (1995) Nonselective and efficient fluorescent labeling of glycans using 2-amino benzamide and anthranilic acid. Anal Biochem 230:229–238

Bremer B, Bremer K, Chase M, Fay M, Reveal J, Soltis D, Soltis P, Stevens P (2009) An update of the Angiosperm Phylogeny Group classification for the orders and families of flowering plants: APG III. Bot J Linnean Soc 161:105–121

Buanafina M (2009) Feruloylation in grasses: current and future perspectives. Mol Plant 2:861–872

Carnachan SM, Harris PJ (2000) Polysaccharide compositions of primary cell walls of the palms *Phoenix canariensis* and *Rhopalostylis sapida*. Plant Physiol Biochem 38:699–708

Carpita NC (1996) Structure and biogenesis of the cell walls of grasses. Annu Rev Plant Biol 47:445–476

Carpita NC, Gibeaut DM (1993) Structural models of primary cell walls in flowering plants: consistency of molecular structure with the physical properties of the walls during growth. Plant J 3:1–30

Chase M, Soltis DE, Olmstead RG, Morgan D, Les D, Mishler BD, Duvall MR, Price RA, Hills HG, Qiu Y-L (1993) Phylogenetics of seed plants: an analysis of nucleotide sequences from the plastid gene rbcL. Ann Mo Bot Garden 80:528–580

Chase M, Fay MF, Devey DS, Maurin O, Rønsted N, Davies TJ, Pillon Y, Petersen G, Seberg O, Tamura M (2006) Multigene analyses of monocot relationships: a summary. Aliso 22:63–75

Chong S-L, Koutaniemi S, Juvonen M, Derba-Maceluch M, Mellerowicz EJ, Tenkanen M (2015) Glucuronic acid in *Arabidopsis thaliana* xylans carries a novel pentose substituent. Int J Biol Macromol 79:807–812

Darvill JE, McNeil M, Darvill AG, Albersheim P (1980) Structure of plant cell walls: XI. Glucuronoarabinoxylan, a second hemicellulose in the primary cell walls of suspension-cultured sycamore cells. Plant Physiol 66:1135–1141

Domon B, Costello C (1988) A systematic nomenclature for carbohydrate fragmentations in FAB-MS/MS spectra of glycoconjugates. Glycoconjug J 5:397–409

Ebringerova A, Hromadkova Z, Heinze T (2005) Hemicellulose. Adv Polym Sci 186:1–67

Fangel J, Ulvskov P, Knox JP, Mikkelsen M, Harholt J, Popper Z, Willats W (2012) Cell wall evolution and diversity. Front Plant Sci 3:1–8

Gibeaut DM, Pauly M, Bacic A, Fincher GB (2005) Changes in cell wall polysaccharides in developing barley (*Hordeum vulgare*) coleoptiles. Planta 221:729–738

Givnish TJ, Ames M, McNeal J, McKain MR, Steele PR, dePamphilis CW, Graham SW, Pires JC, Stevenson D, Zomlefer W (2010) Assembling the tree of the monocotyledons: plastome sequence phylogeny and evolution of Poales. Ann Mo Bot Garden 97:584–616

Glushka JN, Terrell M, York WS, O'Neill MA, Gucwa A, Darvill AG, Albersheim P, Prestegard JH (2003) Primary structure of the 2-*O*-methyl-α-fucose-containing side chain of the pectic polysaccharide, rhamnogalacturonan II. Carbohydr Res 338:341–352

Harris P (2006) Primary and secondary plant cell walls: a comparative overview. N Zeal J For Sci 36:36–53

Harris PJ, Hartley R (1980) Phenolic constituents of the cell walls of monocotyledons. Biochem Syst Ecol 8:153–160

Harris PJ, Trethewey J (2010) The distribution of ester-linked ferulic acid in the cell walls of angiosperms. Phytochem Rev 9:19–33

Harris PJ, Kelderman MR, Kendon MF, McKenzie RJ (1997) Monosaccharide compositions of unlignified cell walls of monocotyledons in relation to the occurrence of wall-bound ferulic acid. Biochem Syst Ecol 25:167–179

Hervé C, Rogowski A, Gilbert HJ, Knox JP (2009) Enzymatic treatments reveal differential capacities for xylan recognition and degradation in primary and secondary plant cell walls. Plant J 58:413–422

Hsieh YSY, Harris PJ (2009) Xyloglucans of monocotyledons have diverse structures. Mol Plant 2:943–965

Ishii T, Konishi T, Ono H, Ohnishi-Kameyama M, Togashi H, Shimizu K (2008) Assignment of the 1H and 13C NMR spectra of 2-aminobenzamide-labeled xylo-oligosaccharides. Carbohydr Polym 74:579–589

Johansson M, Samuelson O (1977) Reducing end groups in brich xylan and their alkaline degradation. Wood Sci Technol 11:251–263

Kulkarni AR, Pattathil S, Hahn M, York W, O'Neill MA (2012a) Comparison of arabinoxylan structure in bioenergy and model grasses. Ind Biotechnol 8:222–229

Kulkarni AR, Peña MJ, Avci U, Mazumder K, Urbanowicz B, Pattathil S, Yin Y, O'Neill MA, Roberts AW, Hahn MG (2012b) The ability of land plants to synthesize glucuronoxylans predates the evolution of tracheophytes. Glycobiology 22:439–451

Lampugnani E, Moller I, Cassin A, Jones D, Koh PL, Ratnayake S, Beahan C, Wilson SM, Bacic A, Newbigin E (2013) In vitro grown pollen tubes of *Nicotiana alata* actively synthesise a fucosylated xyloglucan. PLoS One 8:e77140

Landolt E (1986) Biosystematic investigation in the family of duckweeds ("Lemnaceae"). The family of "Lemnaceae": a monographic study, vol 2. Veröffentlichungen des Geobotanischen Institutes der ETH, Zürich

Liu L, Paulitz J, Pauly M (2015) The presence of fucogalactoxyloglucan and its synthesis in rice indicates conserved functional importance in plants. Plant Physiol 168:549–560

Mazumder K, York W (2010) Structural analysis of arabinoxylans isolated from ball milled switchgrass biomass. Carbohydr Res 345:2183–2193

Mortimer JC, Faria-Blanc N, Yu X, Tryfona T, Sorieul M, Ng YZ, Zhang Z, Stott K, Anders N, Dupree P (2015) An unusual xylan in Arabidopsis primary cell walls is synthesised by GUX3, IRX9L, IRX10L and IRX14. Plant J 83:413–426

Packer NH, Lawson MA, Jardine DR, Redmond JW (1998) A general approach to desalting oligosaccharides released from glycoproteins. Glycoconjug J 15:737–747

Peña MJ, Zhong R, Zhou GK, Richardson EA, O'Neill MA, Darvill AG, York WS, Ye ZH (2007) Arabidopsis *irregular xylem8* and *irregular xylem9*: implications for the complexity of glucuronoxylan biosynthesis. Plant Cell 19:549–563

Peña MJ, Darvill AG, Eberhard S, York WS, O'Neill MA (2008) Moss and liverwort xyloglucans contain galacturonic acid and are structurally distinct from the xyloglucans synthesized by hornworts and vascular plants. Glycobiology 18:891–899

Peña MJ, Kong Y, York WS, O'Neill MA (2012) A galacturonic acid-containing xyloglucan is involved in Arabidopsis root hair tip growth. Plant Cell 24:4511–4524

Ratnayake S, Beahan CT, Callahan DL, Bacic A (2014) The reducing end sequence of wheat endosperm cell wall arabinoxylans. Carbohydr Res 386:23–32

Reis A, Pinto P, Evtuguin D, Neto CP, Domingues P, Ferrer-Correia A, Domingues MRM (2005) Electrospray tandem mass spectrometry of underivatised acetylated xylo-oligosaccharides. Rapid Comm Mass Spectrom 19:3589–3599

Saulnier L, Vigouroux J, Thibault J-F (1995) Isolation and partial characterization of feruloylated oligosaccharides from maize bran. Carbohydr Res 272:241–253

Shatalov AA, Evtuguin DV, Pascoal Neto C (1999) (2-*O*-α-D-Galactopyranosyl-4-*O*-methyl-α-D-glucurono)-D-xylan from *Eucalyptus globulus* Labill. Carbohydr Res 320:93–99

Smith SA, Donoghue MJ (2008) Rates of molecular evolution are linked to life history in flowering plants. Science 322:86–89

Smith B, Harris P (1999) The polysaccharide composition of Poales cell walls: Poaceae cell walls are not unique. Biochem Syst Ecol 27:33–53

Togashi H, Kato A, Shimizu K (2009) Enzymatically derived aldouronic acids from *Eucalyptus globulus* glucuronoxylan. Carbohydr Polym 78:247–252

Urbanowicz BR, Peña MJ, Ratnaparkhe S, Avci U, Backe J, Steet HF, Foston M, Li H, O'Neill MA, Ragauskas AJ, Darvill AG, Wyman C, Gilbert HJ, York WS (2012) 4-*O*-methylation of glucuronic acid in *Arabidopsis* glucuronoxylan is catalyzed by a domain of unknown function family 579 protein. Proc Nat Acad Sci USA 109:14253–14258

York WS, O'Neill MA (2008) Biochemical control of xylan biosynthesis—which end is up? Curr Opin Plant Biol 11:258–265

Zablackis E, Huang J, Muller B, Darvill AG, Albersheim P (1995) Characterization of the cell-wall polysaccharides of *Arabidopsis thaliana* leaves. Plant Physiol 107:1129–1138

Zhong R, Teng Q, Lee C, Ye Z-H (2014) Identification of a disaccharide side chain 2-*O*-α-D-galactopyranosyl-α-D-glucuronic acid in Arabidopsis xylan. Plant Signal Behav 9:e27933